

Joint LIGO and TAMA300 search for gravitational waves from inspiralling neutron star binaries

B. Abbott,¹ R. Abbott,¹ R. Adhikari,¹ A. Ageev,^{2,3} J. Agresti,¹ P. Ajith,⁴ B. Allen,⁵ J. Allen,⁶ R. Amin,⁷ S. B. Anderson,¹ W. G. Anderson,⁸ M. Araya,¹ H. Armandula,¹ M. Ashley,⁹ F. Asiri,^{1,a} P. Aufmuth,¹⁰ C. Aulbert,¹¹ S. Babak,¹² R. Balasubramanian,¹² S. Ballmer,⁶ B. C. Barish,¹ C. Barker,¹³ D. Barker,¹³ M. Barnes,^{1,b} B. Barr,¹⁴ M. A. Barton,¹ K. Bayer,⁶ R. Beausoleil,^{15,c} K. Belczynski,¹⁶ R. Bennett,^{14,d} S. J. Berukoff,^{11,e} J. Betzwieser,⁶ B. Bhawal,¹ I. A. Bilenko,² G. Billingsley,¹ E. Black,¹ K. Blackburn,¹ L. Blackburn,⁶ B. Bland,¹³ B. Bochner,^{6,f} L. Bogue,¹⁷ R. Bork,¹ S. Bose,¹⁸ P. R. Brady,⁵ V. B. Braginsky,² J. E. Brau,¹⁹ D. A. Brown,¹ A. Bullington,¹⁵ A. Bunkowski,^{4,10} A. Buonanno,²⁰ R. Burgess,⁶ D. Busby,¹ W. E. Butler,²¹ R. L. Byer,¹⁵ L. Cadonati,⁶ G. Cagnoli,¹⁴ J. B. Camp,²² J. Cannizzo,²² K. Cannon,⁵ C. A. Cantley,¹⁴ J. Cao,⁶ L. Cardenas,¹ K. Carter,¹⁷ M. M. Casey,¹⁴ J. Castiglione,²³ A. Chandler,¹ J. Chapsky,^{1,b} P. Charlton,^{1,g} S. Chatterji,¹ S. Chelkowski,^{4,10} Y. Chen,¹¹ V. Chickarmane,^{7,h} D. Chin,²⁴ N. Christensen,²⁵ D. Churches,¹² T. Cokelaer,¹² C. Colacino,²⁶ R. Coldwell,²³ M. Coles,^{17,i} D. Cook,¹³ T. Corbitt,⁶ D. Coyne,¹ J. D. E. Creighton,⁵ T. D. Creighton,¹ D. R. M. Crooks,¹⁴ P. Csatorday,⁶ B. J. Cusack,²⁷ C. Cutler,¹¹ J. Dalrymple,³ E. D'Ambrosio,¹ K. Danzmann,^{4,10} G. Davies,¹² E. Daw,^{7,j} D. DeBra,¹⁵ T. Delker,^{23,k} V. Dergachev,²⁴ S. Desai,⁹ R. DeSalvo,¹ S. Dhurandhar,²⁸ A. Di Credico,³ M. Díaz,⁸ H. Ding,¹ R. W. P. Drever,²⁹ R. J. Dupuis,¹ J. A. Edlund,^{1,b} P. Ehrens,¹ E. J. Elliffe,¹⁴ T. Etzel,¹ M. Evans,¹ T. Evans,¹⁷ S. Fairhurst,⁵ C. Fallnich,¹⁰ D. Farnham,¹ M. M. Fejer,¹⁵ T. Findley,³⁰ M. Fine,¹ L. S. Finn,⁹ K. Y. Franzen,²³ A. Freise,^{4,l} R. Frey,¹⁹ P. Fritschel,⁶ V. V. Frolov,¹⁷ M. Fyffe,¹⁷ K. S. Ganezer,³¹ J. Garofoli,¹³ J. A. Giaime,⁷ A. Gillespie,^{1,m} K. Goda,⁶ L. Goggin,¹ G. González,⁷ S. Goßler,¹⁰ P. Grandclément,^{16,n} A. Grant,¹⁴ C. Gray,¹³ A. M. Gretarsson,³² D. Grimmitt,¹ H. Grote,⁴ S. Grunewald,¹¹ M. Guenther,¹³ E. Gustafson,^{15,o} R. Gustafson,²⁴ W. O. Hamilton,⁷ M. Hammond,¹⁷ C. Hanna,⁷ J. Hanson,¹⁷ C. Hardham,¹⁵ J. Harms,³³ G. Harry,⁶ A. Hartunian,¹ J. Heefner,¹ Y. Hefetz,⁶ G. Heinzel,⁴ I. S. Heng,¹⁰ M. Hennessy,¹⁵ N. Hepler,⁹ A. Heptonstall,¹⁴ M. Heurs,¹⁰ M. Hewitson,⁴ S. Hild,⁴ N. Hindman,¹³ P. Hoang,¹ J. Hough,¹⁴ M. Hrynevych,^{1,p} W. Hua,¹⁵ M. Ito,¹⁹ Y. Itoh,¹¹ A. Ivanov,¹ O. Jennrich,^{14,q} B. Johnson,¹³ W. W. Johnson,⁷ W. R. Johnston,⁸ D. I. Jones,⁹ G. Jones,¹² L. Jones,¹ D. Jungwirth,^{1,r} V. Kalogera,¹⁶ E. Katsavounidis,⁶ K. Kawabe,¹³ W. Kells,¹ J. Kern,^{17,s} A. Khan,¹⁷ S. Killbourn,¹⁴ C. J. Killow,¹⁴ C. Kim,¹⁶ C. King,¹ P. King,¹ S. Klimenko,²³ S. Koranda,⁵ K. Kötter,¹⁰ J. Kovalik,^{17,b} D. Kozak,¹ B. Krishnan,¹¹ M. Landry,¹³ J. Langdale,¹⁷ B. Lantz,¹⁵ R. Lawrence,⁶ A. Lazzarini,¹ M. Lei,¹ I. Leonor,¹⁹ K. Libbrecht,¹ A. Libson,²⁵ P. Lindquist,¹ S. Liu,¹ J. Logan,^{1,t} M. Lormand,¹⁷ M. Lubinski,¹³ H. Lück,^{4,10} M. Luna,³⁴ T. T. Lyons,^{1,t} B. Machenschalk,¹¹ M. MacInnis,⁶ M. Mageswaran,¹ K. Mailand,¹ W. Majid,^{1,b} M. Malec,^{4,10} V. Mandic,¹ F. Mann,¹ A. Marin,^{6,u} S. Márka,³⁵ E. Maros,¹ J. Mason,^{1,v} K. Mason,⁶ O. Matherny,¹³ L. Matone,³⁵ N. Mavalvala,⁶ R. McCarthy,¹³ D. E. McClelland,²⁷ M. McHugh,³⁶ J. W. C. McNabb,⁹ A. Melissinos,²¹ G. Mendell,¹³ R. A. Mercer,²⁶ S. Meshkov,¹ E. Messaritaki,⁵ C. Messenger,²⁶ E. Mikhailov,⁶ S. Mitra,²⁸ V. P. Mitrofanov,² G. Mitselmakher,²³ R. Mittleman,⁶ O. Miyakawa,¹ S. Mohanty,⁸ G. Moreno,¹³ K. Mossavi,⁴ G. Mueller,²³ S. Mukherjee,⁸ P. Murray,¹⁴ E. Myers,³⁷ J. Myers,¹³ S. Nagano,⁴ T. Nash,¹ R. Nayak,²⁸ G. Newton,¹⁴ F. Nocera,¹ J. S. Noel,¹⁸ P. Nutzman,¹⁶ T. Olson,³⁸ B. O'Reilly,¹⁷ D. J. Ottaway,⁶ A. Ottewill,^{5,w} D. Ouimette,^{1,r} H. Overmier,¹⁷ B. J. Owen,⁹ Y. Pan,³⁹ M. A. Papa,¹¹ V. Parameshwaraiah,¹³ C. Parameshwaraiah,¹⁷ M. Pedraza,¹ S. Penn,⁴⁰ M. Pitkin,¹⁴ M. Plissi,¹⁴ R. Prix,¹¹ V. Quetschke,²³ F. Raab,¹³ H. Radkins,¹³ R. Rahkola,¹⁹ M. Rakhmanov,²³ S. R. Rao,¹ K. Rawlins,^{6,x} S. Ray-Majumder,⁵ V. Re,²⁶ D. Redding,^{1,b} M. W. Regehr,^{1,b} T. Regimbau,¹² S. Reid,¹⁴ K. T. Reilly,¹ K. Reithmaier,¹ D. H. Reitze,²³ S. Richman,^{6,y} R. Riesen,¹⁷ K. Riles,²⁴ B. Rivera,¹³ A. Rizzi,^{17,z} D. I. Robertson,¹⁴ N. A. Robertson,^{14,15} C. Robinson,¹² L. Robison,¹ S. Roddy,¹⁷ A. Rodriguez,⁷ J. Rollins,³⁵ J. D. Romano,¹² J. Romie,¹ H. Rong,^{23,m} D. Rose,¹ E. Rotthoff,⁹ S. Rowan,¹⁴ A. Rüdiger,⁴ L. Ruet,⁶ P. Russell,¹ K. Ryan,¹³ I. Salzman,¹ V. Sandberg,¹³ G. H. Sanders,^{1,aa} V. Sannibale,¹ P. Sarin,⁶ B. Sathyaprakash,¹² P. R. Saulson,³ R. Savage,¹³ A. Sazonov,²³ R. Schilling,⁴ K. Schlaufman,⁹ V. Schmidt,^{1,bb} R. Schnabel,³³ R. Schofield,¹⁹ B. F. Schutz,^{11,12} P. Schwinberg,¹³ S. M. Scott,²⁷ S. E. Seader,¹⁸ A. C. Searle,²⁷ B. Sears,¹ S. Seel,¹ F. Seifert,³³ D. Sellers,¹⁷ A. S. Sengupta,²⁸ C. A. Shapiro,^{9,cc} P. Shawhan,¹ D. H. Shoemaker,⁶ Q. Z. Shu,^{23,dd} A. Sibley,¹⁷ X. Siemens,⁵ L. Sievers,^{1,b} D. Sigg,¹³ A. M. Sintes,^{11,34} J. R. Smith,⁴ M. Smith,⁶ M. R. Smith,¹ P. H. Sneddon,¹⁴ R. Spero,^{1,b} O. Spjeld,¹⁷ G. Stapfer,¹⁷ D. Steussy,²⁵ K. A. Strain,¹⁴ D. Strom,¹⁹ A. Stuver,⁹ T. Summerscales,⁹ M. C. Sumner,¹ M. Sung,⁷ P. J. Sutton,¹ J. Sylvestre,^{1,ee} D. B. Tanner,²³ H. Tariq,¹ M. Tarallo,¹ I. Taylor,¹² R. Taylor,¹⁴ R. Taylor,¹ K. A. Thorne,⁹ K. S. Thorne,³⁹ M. Tibbits,⁹ S. Tilav,^{1,ff} M. Tinto,^{29,b} K. V. Tokmakov,² C. Torres,⁸ C. Torrie,¹ G. Traylor,¹⁷ W. Tyler,¹ D. Ugolini,⁴¹ C. Ungarelli,²⁶ M. Vallisneri,^{39,gg} M. van Putten,⁶ S. Vass,¹ A. Vecchio,²⁶ J. Veitch,¹⁴ C. Vorvick,¹⁴ S. P. Vyachanin,² L. Wallace,¹ H. Walther,³³ H. Ward,¹⁴ R. Ward,¹ B. Ware,^{1,b} K. Watts,¹⁷ D. Webber,¹ A. Weidner,^{33,4} U. Weiland,¹⁰ A. Weinstein,¹ R. Weiss,⁶ H. Welling,¹⁰ L. Wen,¹¹ S. Wen,⁷ K. Wette,²⁷ J. T. Whelan,³⁶ S. E. Whitcomb,¹ B. F. Whiting,²³ S. Wiley,³¹ C. Wilkinson,¹³ P. A. Willems,¹ P. R. Williams,^{11,hh} R. Williams,²⁹ B. Willke,^{4,10} A. Wilson,¹ B. J. Winjum,^{9,e}

W. Winkler,⁴ S. Wise,²³ A. G. Wiseman,⁵ G. Woan,¹⁴ D. Woods,⁵ R. Wooley,¹⁷ J. Worden,¹³ W. Wu,²³ I. Yakushin,¹⁷
 H. Yamamoto,¹ S. Yoshida,³⁰ K. D. Zaleski,⁹ M. Zanolin,⁶ I. Zawischa,^{10,ii} L. Zhang,¹ R. Zhu,¹¹ N. Zotov,⁴²
 M. Zucker,¹⁷ and J. Zweizig¹

(LIGO Scientific Collaboration, <http://www.ligo.org>)

¹LIGO-California Institute of Technology, Pasadena, California 91125, USA

²Moscow State University, Moscow, 119992, Russia

³Syracuse University, Syracuse, New York 13244, USA

⁴Albert-Einstein-Institut, Max-Planck-Institut für Gravitationsphysik, D-30167 Hannover, Germany

⁵University of Wisconsin-Milwaukee, Milwaukee, Wisconsin 53201, USA

⁶LIGO-Massachusetts Institute of Technology, Cambridge, Massachusetts 02139, USA

⁷Louisiana State University, Baton Rouge, Louisiana 70803, USA

⁸The University of Texas at Brownsville and Texas Southmost College, Brownsville, Texas 78520, USA

⁹The Pennsylvania State University, University Park, Pennsylvania 16802, USA

¹⁰Universität Hannover, D-30167 Hannover, Germany

¹¹Albert-Einstein-Institut, Max-Planck-Institut für Gravitationsphysik, D-14476 Golm, Germany

¹²Cardiff University, Cardiff, CF2 3YB, United Kingdom

¹³LIGO Hanford Observatory, Richland, Washington 99352, USA

¹⁴University of Glasgow, Glasgow, G12 8QQ, United Kingdom

¹⁵Stanford University, Stanford, California 94305, USA

¹⁶Northwestern University, Evanston, Illinois 60208, USA

¹⁷LIGO Livingston Observatory, Livingston, Louisiana 70754, USA

¹⁸Washington State University, Pullman, Washington 99164, USA

¹⁹University of Oregon, Eugene, Oregon 97403, USA

²⁰University of Maryland, College Park, Maryland 20742 USA

²¹University of Rochester, Rochester, New York 14627, USA

²²NASA/Goddard Space Flight Center, Greenbelt, Maryland 20771, USA

²³University of Florida, Gainesville, Florida 32611, USA

²⁴University of Michigan, Ann Arbor, Michigan 48109, USA

²⁵Carleton College, Northfield, Minnesota 55057, USA

²⁶University of Birmingham, Birmingham, B15 2TT, United Kingdom

²⁷Australian National University, Canberra, 0200, Australia

²⁸Inter-University Centre for Astronomy and Astrophysics, Pune-411007, India

²⁹California Institute of Technology, Pasadena, California 91125, USA

³⁰Southeastern Louisiana University, Hammond, Louisiana 70402, USA

³¹California State University Dominguez Hills, Carson, California 90747, USA

³²Embry-Riddle Aeronautical University, Prescott, Arizona 86301 USA

³³Max Planck Institut für Quantenoptik, D-85748, Garching, Germany

³⁴Universitat de les Illes Balears, E-07122 Palma de Mallorca, Spain

³⁵Columbia University, New York, New York 10027, USA

³⁶Loyola University, New Orleans, Louisiana 70118, USA

³⁷Vassar College, Poughkeepsie, New York 12604, USA

³⁸Salish Kootenai College, Pablo, Montana 59855, USA

³⁹Caltech-CaRT, Pasadena, California 91125, USA

⁴⁰Hobart and William Smith Colleges, Geneva, New York 14456, USA

⁴¹Trinity University, San Antonio, Texas 78212, USA

⁴²Louisiana Tech University, Ruston, Louisiana 71272, USA

T. Akutsu,⁴³ T. Akutsu,⁴⁴ M. Ando,⁴⁵ K. Arai,⁴⁶ A. Araya,⁴⁷ H. Asada,⁴⁸ Y. Aso,⁴⁵ P. Beyersdorf,⁴⁶ Y. Fujiki,⁴⁹
 M.-K. Fujimoto,⁴⁶ R. Fujita,⁵⁰ M. Fukushima,⁴⁶ T. Futamase,⁵¹ Y. Hamuro,⁴⁹ T. Haruyama,⁵² K. Hayama,⁴⁶ H. Iguchi,⁵³
 Y. Iida,⁴⁵ K. Ioka,⁵⁷ H. Ishitsuka,⁴³ N. Kamikubota,⁵² N. Kanda,⁵⁴ T. Kaneyama,⁴⁹ Y. Karasawa,⁵¹ K. Kasahara,⁴³
 T. Kasai,⁴⁸ M. Katsuki,⁵⁴ S. Kawamura,⁴⁶ M. Kawamura,⁴⁹ F. Kawazoe,⁵⁵ Y. Kojima,⁵⁶ K. Kokeyama,⁵⁵ K. Kondo,⁴³
 Y. Kozai,⁴⁶ H. Kudoh,⁴⁵ K. Kuroda,⁴³ T. Kuwabara,⁴⁹ N. Matsuda,⁵⁸ N. Mio,⁵⁹ K. Miura,⁶⁰ S. Miyama,⁴⁶ S. Miyoki,⁴³
 H. Mizusawa,⁴⁹ S. Moriwaki,⁵⁹ M. Musha,⁶¹ Y. Nagayama,⁵⁴ K. Nakagawa,⁶¹ T. Nakamura,⁵⁷ H. Nakano,⁵⁴ K. Nakao,⁵⁴
 Y. Nishi,⁴⁵ K. Numata,⁴⁵ Y. Ogawa,⁵² M. Ohashi,⁴³ N. Ohishi,⁴⁶ A. Okutomi,⁴³ K. Oohara,⁴⁹ S. Otsuka,⁴⁵ Y. Saito,⁵²
 S. Sakata,⁵⁵ M. Sasaki,⁶⁶ N. Sato,⁵² S. Sato,⁴⁶ Y. Sato,⁶¹ K. Sato,⁶² A. Sekido,⁶³ N. Seto,⁵⁰ M. Shibata,⁶⁴ H. Shinkai,⁶⁵
 T. Shintomi,⁵² K. Soida,⁴⁵ K. Somiya,⁵⁹ T. Suzuki,⁵² H. Tagoshi,⁵⁰ H. Takahashi,⁴⁹ R. Takahashi,⁴⁶ A. Takamori,⁴⁷

S. Takemoto,⁵⁷ K. Takeno,⁵⁹ T. Tanaka,⁶⁶ K. Taniguchi,⁶⁹ T. Tanji,⁵⁹ D. Tatsumi,⁴⁶ S. Telada,⁶⁸ M. Tokunari,⁴³ T. Tomaru,⁵² K. Tsubono,⁴⁵ N. Tsuda,⁶² Y. Tsunesada,⁴⁶ T. Uchiyama,⁴³ K. Ueda,⁶¹ A. Ueda,⁴⁶ K. Waseda,⁴⁶ A. Yamamoto,⁵² K. Yamamoto,⁴³ T. Yamazaki,⁴⁶ Y. Yanagi,⁵⁵ J. Yokoyama,⁶⁷ T. Yoshida,⁵¹ and Z.-H. Zhu⁴⁶

(TAMA Collaboration)

⁴³*Institute for Cosmic Ray Research, The University of Tokyo, Kashiwa, Chiba 277-8582, Japan*

⁴⁴*Department of Astronomy, The University of Tokyo, Bunkyo-ku, Tokyo 113-0033, Japan*

⁴⁵*Department of Physics, The University of Tokyo, Bunkyo-ku, Tokyo 113-0033, Japan*

⁴⁶*National Astronomical Observatory of Japan, Tokyo 181-8588, Japan*

⁴⁷*Earthquake Research Institute, The University of Tokyo, Bunkyo-ku, Tokyo 113-0032, Japan*

⁴⁸*Faculty of Science and Technology, Hirosaki University, Hirosaki, Aomori 036-8561, Japan*

⁴⁹*Faculty of Science, Niigata University, Niigata, Niigata 950-2102, Japan*

⁵⁰*Graduate School of Science, Osaka University, Toyonaka, Osaka 560-0043, Japan*

⁵¹*Graduate School of Science, Tohoku University, Sendai, Miyagi 980-8578, Japan*

⁵²*High Energy Accelerator Research Organization, Tsukuba, Ibaraki 305-0801, Japan*

⁵³*Tokyo Institute of Technology, Meguro-ku, Tokyo 152-8551, Japan*

⁵⁴*Graduate School of Science, Osaka City University, Sumiyoshi-ku, Osaka 558-8585, Japan*

⁵⁵*Ochanomizu University, Bunkyo-ku, Tokyo 112-8610, Japan*

⁵⁶*Department of Physics, Hiroshima University, Higashi-Hiroshima, Hiroshima 739-8526, Japan*

⁵⁷*Faculty of Science, Kyoto University, Sakyo-ku, Kyoto 606-8502, Japan*

⁵⁸*Tokyo Denki University, Chiyoda-ku, Tokyo 101-8457, Japan*

⁵⁹*Department of Advanced Materials Science, The University of Tokyo, Kashiwa, Chiba 277-8561, Japan*

⁶⁰*Department of Physics, Miyagi University of Education, Aoba Aramaki, Sendai 980-0845, Japan*

⁶¹*Institute for Laser Science, University of Electro-Communications, Chofugaoka, Chofu, Tokyo 182-8585, Japan*

⁶²*Precision Engineering Division, Faculty of Engineering, Tokai University, Hiratsuka, Kanagawa 259-1292, Japan*

⁶³*Waseda University, Shinjyuku-ku, Tokyo 169-8555, Japan*

⁶⁴*Graduate School of Arts and Sciences, The University of Tokyo, Meguro-ku, Tokyo 153-8902, Japan*

⁶⁵*RIKEN, Wako, Saitaka 351-0198, Japan*

⁶⁶*Yukawa Institute for Theoretical Physics, Kyoto University, Sakyo-ku, Kyoto 606-8502, Japan*

⁶⁷*Research Center for the Early Universe (RESCEU), Graduate School of Science, The University of Tokyo, Tokyo 113-0033, Japan*

⁶⁸*National Institute of Advanced Industrial Science and Technology, Tsukuba, Ibaraki 305-8563, Japan*

⁶⁹*Department of Physics, University of Illinois at Urbana-Champaign, Urbana, Illinois 61801, USA*

(Received 11 January 2006; published 16 May 2006)

We search for coincident gravitational wave signals from inspiralling neutron star binaries using LIGO and TAMA300 data taken during early 2003. Using a simple trigger exchange method, we perform an intercollaboration coincidence search during times when TAMA300 and only one of the LIGO sites were operational. We find no evidence of any gravitational wave signals. We place an observational upper limit on the rate of binary neutron star coalescence with component masses between 1 and $3M_{\odot}$ of 49 per year

^cPermanent Address: HP Laboratories

^dCurrently at Rutherford Appleton Laboratory

^eCurrently at University of CA, Los Angeles, USA

^fCurrently at Hofstra University

^gCurrently at Charles Sturt University, Australia

^hCurrently at Keck Graduate Institute

ⁱCurrently at National Science Foundation

^jCurrently at University of Sheffield

^kCurrently at Ball Aerospace Corporation

^lCurrently at European Gravitational Observatory

^mCurrently at Intel Corp.

ⁿCurrently at University of Tours, France

^oCurrently at Lightconnect Inc.

^pCurrently at W. M. Keck Observatory

^qCurrently at ESA Science and Technology Center

^rCurrently at Raytheon Corporation

^sCurrently at NM Institute of Mining and Technology/
Magdalena Ridge Observatory Interferometer, USA

^tCurrently at Mission Research Corporation

^uCurrently at Harvard University

^vCurrently at Lockheed-Martin Corporation

^wPermanent Address: University College Dublin

^xCurrently at University of AK Anchorage, USA

^yCurrently at Research Electro-Optics Inc.

^zCurrently at Institute of Advanced Physics, Baton Rouge, LA,
USA

^{aa}Currently at Thirty Meter Telescope Project at Caltech

^{bb}Currently at European Commission, DG Research, Brussels,
Belgium

^{cc}Currently at University of Chicago

^{dd}Currently at LightBit Corporation

^{ee}Permanent Address: IBM Canada Ltd.

^{ff}Currently at University of DE, USA

^{gg}Permanent Address: Jet Propulsion Laboratory

^{hh}Currently at Shanghai Astronomical Observatory

ⁱⁱCurrently at Laser Zentrum Hannover

^{jj}Currently at Shanghai Astronomical Observatory

^{kk}Currently at Laser Zentrum Hannover

per Milky Way equivalent galaxy at a 90% confidence level. The methods developed during this search will find application in future network inspiral analyses.

DOI: [10.1103/PhysRevD.73.102002](https://doi.org/10.1103/PhysRevD.73.102002)

PACS numbers: 95.85.Sz, 04.80.Nn, 07.05.Kf, 95.55.Ym

The first generation of gravitational wave interferometric detectors are rapidly approaching their design sensitivities. These include the LIGO [1] and TAMA300 [2] detectors as well as GEO [3] and Virgo [4]. Inspiralling binaries of neutron stars and/or black holes are one of the most promising sources of gravitational radiation for these detectors. Indeed, several searches for such signals have already been completed [5–8]. In the long term, the chances of detecting gravitational waves from a binary inspiral are greatly improved by making optimal use of data from all available detectors. The immediate benefit of a multi-detector coincidence search is a significant reduction in the false alarm rate for a fixed detection efficiency. Additionally, a search involving all available detectors will provide an increase in observation time when, for example, at least two detectors are operating. The different orientations of the detectors make them sensitive to different parts of the sky, thus a combined search can lead to improved sky coverage. If an event is detected in multiple instruments it is possible to localize the position of the source and improve parameter estimation. In addition, independent observations in well-separated detectors using different hardware and analysis algorithms would increase confidence in a detection, while reducing the possibility of an error or bias.

The importance of joint searches has long been acknowledged, and indeed several network searches have previously been completed. A network of resonant detectors was used to carry out a joint search for gravitational wave bursts [9], and more recently data from the LIGO and TAMA300 detectors were used to perform a joint burst search [10]. In this paper, we present the first intercollaboration search for gravitational waves from the binary inspiral of neutron stars using modern large scale interferometric detectors. This represents an important step towards a global network analysis of gravitational wave data. Furthermore, this search provides a firm basis for development of network analysis techniques.

The joint coincidence search described here uses data from the second LIGO science run (S2) which occurred at the same time as the eighth TAMA300 data taking run (DT8) in 2003. The LIGO S2 data have already been searched for gravitational waves from binary neutron stars [7]. That search used only data in which both of the LIGO sites were operational. In this paper, we report on a coincidence search using LIGO and TAMA300 data when only one LIGO site was operating in coincidence with the TAMA300 detector. The LIGO data analyzed in this paper was not analyzed in Ref. [7]. During S2 and DT8, the LIGO detectors were an order of magnitude more sensitive

than TAMA300. However, since TAMA300 was sensitive to the majority of candidate sources in the Milky Way, a joint coincidence search provides information about inspiralling neutron star binaries in the galaxy. Further, by performing this joint search between the LIGO and TAMA collaborations, we are able to significantly increase the length of time searched in coincidence during the S2/DT8 run. Since LIGO and TAMA300 were the only large interferometers which were operated during S2/DT8 period, it is important to perform a joint analysis.

The data from each of the detectors are searched independently for event candidates, or “triggers” [9]. The details of these triggers, such as the coalescence time and the masses of the component stars, are then exchanged between collaboration members, and the triggers are searched for coincidences. The coincidence requirements of the search are determined by adding simulated signals to the data streams of the detectors, and determining the accuracy with which various parameters are recovered [11]. The exchange of single instrument triggers and subsequent coincidence analysis is quite simple and does not involve the exchange of large amounts of interferometer data. It provides a natural first step in an intercollaboration analysis. If an interesting candidate event were found, it would then be followed up by an optimal, fully coherent analysis of the data around the time of the candidate. In this joint LIGO-TAMA300 search, we find no evidence of any inspiral signals in the data and so we place an observational upper limit on the rate of binary neutron star coalescence in the Milky Way galaxy.

The LIGO network of detectors consists of a 4 km interferometer “L1” in Livingston, LA and a 4 km “H1” and a 2 km “H2” interferometer which share a common vacuum system in Hanford, WA. TAMA300 is a 300 m interferometer “T1” in Mitaka, Tokyo. Basic information on the position and orientation of these detectors and detailed descriptions of their operation can be found in Refs. [1,2]. The data analyzed in this search was taken during LIGO S2, TAMA300 DT8 between 16:00 UTC 14 February 2003 and 16:00 UTC 14 April 2003. We only analyze data from the periods when both LIGO and TAMA300 interferometers were operating. Furthermore, we restrict to times when only one of the LIGO sites was operational. Therefore, we have four independent data sets to analyze: the data set during which neither H1 nor H2 were operating—the nH1-nH2-L1-T1 coincident data set (here “n” stands for “not operating”)—and three data sets when one or both of the Hanford detectors were operational but L1 was not—the H1-H2-nL1-T1, H1-nH2-nL1-T1, and nH1-H2-nL1-T1 coincident data sets.

During the S2 science run, a strong correlation was found in the L1 interferometer between inspiral triggers and nonstationary noise in the auxiliary channel, L1:LSC-POB_I, which is proportional to the length fluctuations of the power recycling cavity. Therefore, we apply a veto to exclude times of excess noise in POB_I, details of which are given in Ref. [7]. No efficient veto channels were found for the H1, H2 or T1 detectors. After applying the veto to L1, there are 34 h of nH1-nH2-L1-T1 data. Additionally, there are 334 h of H1-H2-nL1-T1 data, 212 h of H1-nH2-nL1-T1 data and 68 h of nH1-H2-nL1-T1 data, giving a total observation time of 648 h. The data used in this search are summarized in Fig. 1.

To avoid any bias from tuning our pipeline using the same data from which we derive our upper limits, the tuning of analysis parameters was done without examining the full coincident trigger sets. Instead, parameter tuning was done on the *playground* data which consists of approximately 10% of the data chosen as a representative sample. In this analysis, the length of playground data is 64 h. The analysis of the playground data and tuning of the search is described in more detail in Ref. [11]. The playground data was searched for candidate gravitational wave events, but was excluded from the data set used to place the upper limit. Subtracting the playground data leaves a total of 584 h of nonplayground data used in placing the upper limit.

In a search for inspiralling neutron star binaries, we can characterize the sensitivity of the detectors by their maximum observable effective distance, or range. This is defined as the distance at which an inspiral of 1.4–1.4 M_{\odot} neutron stars, in the optimal direction and orientation with respect to each detector, would produce a signal to noise ratio (SNR) of 8. The effective distance of a signal is always greater than or equal to the actual distance. On average it is 2.3 times as large as the actual distance, with

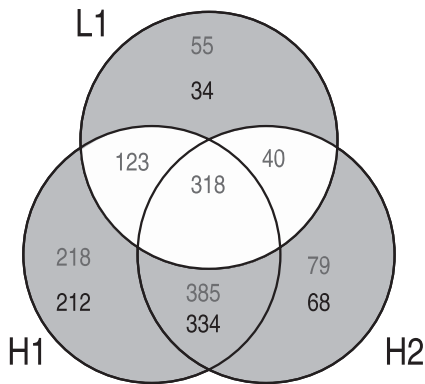


FIG. 1. The number of hours that each combination of detectors was searched during the S2/DT8 run. The upper number gives the amount of time the specific LIGO detectors were coincidentally operational. The lower number gives the total amount of time searched in coincidence with TAMA300. The shaded region corresponds to the data used in this search.

the exact factor dependent upon the source location and orientation relative to the detector. During the S2 science run the ranges of the LIGO detectors, averaged over the course of the run, were 2.0, 0.9 and 0.6 Mpc for L1, H1 and H2, respectively. This made them sensitive to signals from the Milky Way and favorably oriented potential sources in the local group of galaxies. The range of TAMA300 during DT8 was 52 kpc, making it sensitive to the majority of the Milky Way. Thus, the detectors were sensitive to a similar population of candidate sources. Since we require a signal to be observed in both the LIGO and TAMA300 detectors, for this search we restrict our attention to gravitational waves produced by inspiralling neutron star binaries in the Milky Way.

The search methods employed in this paper are similar to those used in the LIGO S2 search [7] and the independent TAMA300 DT8 search [12]. Therefore, in this paper we will not describe the LIGO or TAMA300 analysis pipelines in great detail, but instead emphasize the differences between this search and those described previously.

For the LIGO search, we split the data into analysis blocks of 2048 sec length, overlapped by 128 sec. For each block, we construct a template bank with a minimal match of 97% and component masses between 1 and 3 M_{\odot} [13]. We analyze the data using the FINDCHIRP implementation of matched filtering for inspiral signals in the LIGO Algorithm Library [14,15]. The most important thresholds used in the LIGO search are given in Table I. Most notably, we use a SNR threshold $\rho^* = 7$ for matched filtering. Additionally, we perform a waveform consistency (χ^2) test [16]. For this, we require the power observed in the signal to be evenly distributed between p frequency bands. The threshold is

$$\chi^2 \leq (p + \delta\rho^2)\xi^*. \quad (1)$$

We use a higher threshold on SNR (7 rather than 6) and also a tighter χ^2 threshold (5 rather than 12.5 in the Hanford detectors) than in the LIGO-only S2 inspiral analysis. This is due to the fact that we limit our attention to signals from the Milky Way which tend to have a large SNR in the LIGO S2 data stream. The tighter thresholds vastly reduce the false alarm rate while giving a negligible loss of detection efficiency.

TABLE I. A list of the most significant parameters used for the search of the LIGO data.

Parameter	Description	value
MM	Templatebank minimal match	97%
ρ^*	Matched filter threshold	7.0
p	Number of χ^2 bins	15
δ	χ^2 threshold parameter	0.023
ξ^*	χ^2 threshold parameter	5.0
δt_{HH}	H1/H2 Timing Coincidence	1.0 ms
δm_{HH}	H1/H2 Mass Coincidence	0

For times during which both the H1 and H2 detectors were operational, we perform a triggered analysis of H2, as described in detail in Ref. [7]. We produce a template bank and matched filter the H1 data. Only for those times and masses that we obtain a trigger in H1 do we filter the H2 data. This significantly reduces our analysis time while having no effect on the detection efficiency. We then search for triggers coincident in time and mass between the H1 and H2 detectors. The use of a triggered search allows us to require the mass parameters of coincident triggers to be identical. Studies performed by injecting simulated signals show we can determine the end time of an inspiral to within 1 ms and consequently we use this as our time coincidence window. Finally, we implement an amplitude consistency test between triggers in H1 and H2 [7]; this includes keeping any triggers from H1 whose recovered effective distance renders them unobservable in the less sensitive H2 detector.

For the TAMA300 search, we split the data into analysis blocks of 52.4288 sec length. The adjacent blocks of data are overlapped by 4.0 sec in order not to lose signals which lie on the border of two adjacent blocks. We construct a template bank with a minimal-match of 97% [17] for each locked segment, in which the detector was continuously operated without any interruptions. The most significant thresholds in the TAMA300 search are listed in Table II. We use a SNR threshold $\rho^* = 7$ for matched filtering. In the TAMA300 only search, we introduce a threshold on the value of $\rho/\sqrt{\chi^2}$ to reduce the number of false alarms [12,18]. However, in the LIGO-TAMA300 analysis, we introduce a χ^2 threshold as in Eq. (1). By cutting on χ^2 , the number of triggers is significantly reduced. In addition, some of the coincidence analysis becomes much simpler since LIGO and TAMA300 use a similar criterion for χ^2 . More details of the TAMA300 analysis pipeline are available in Refs. [12,18].

The requirements for coincidence between triggers in the LIGO and TAMA300 detectors are determined by adding simulated inspiral events to the data streams of the detectors. Thresholds are chosen so that injected signals seen separately in both the LIGO and TAMA300 detectors survive the coincidence step with near 100% efficiency, while minimizing the rate of accidental coincidences. Since both the LIGO and TAMA300 pipelines can

accurately determine the coalescence time and mass of an injected signal, it is natural to require consistency of these values in our coincidence test. We measure the accuracy with which these parameters are recovered in each detector and set the coincidence window to be the sum of these accuracies. The values of time and mass coincidence parameters are given in Table III. Both pipelines recover the end time with an accuracy of 1 ms, to which we must add the light travel time between sites to obtain the values given in the table. The mass parameter most accurately recovered by the pipelines is the chirp mass of a signal. The chirp mass is defined as $\mathcal{M} = M\eta^{3/5}$, where $M = m_1 + m_2$ is the total mass of the system and $\eta = m_1 m_2 / M^2$ is the dimensionless mass ratio. To pass coincidence, we require the chirp masses of two triggers to agree within $0.05M_\odot$. Further details of how these parameters were chosen are available in Ref. [11].

The coincidence parameters described above were chosen to provide a good efficiency to simulated events. However, there is some chance that noise induced events in the detectors might survive our coincidence tests. In order to estimate the background of such chance coincident triggers we perform a time-shift analysis [19]. To do this, we time-shift the TAMA300 triggers by multiples of 5 sec and search for coincidence between the time-shifted TAMA300 triggers and LIGO triggers. We perform 100 time-shifts, with a value of the time-shift ranging from -250 to 250 sec. These shifts are much longer than the light travel time between the sites, so that any coincidence cannot be from actual gravitational waves. They are also longer than the typical detector noise autocorrelation time, longer than the longest signal template duration (4 sec) and shorter than typical time scales of detectors' nonstationarity, so that each time-shift provides an independent estimate of the accidental coincident rate. The SNRs of the triggers obtained from the time-shift analysis are plotted in Fig. 2. The plot shows that the distribution of background coincidences does not follow the circular false alarm contours expected for Gaussian noise [20]. Instead, a statistic which more accurately reflects the constant false alarm probability contours is the sum of the SNR in the two detectors,

$$\rho_C = \rho_{\text{LIGO}} + \rho_{\text{TAMA}}. \quad (2)$$

We use this statistic in our analysis to distinguish background triggers from detection candidates.

TABLE II. A list of the most significant parameters used for the search of the TAMA300 data.

Parameter	Description	value
MM	Templatebank minimal match	97%
ρ^*	Matched filter threshold	7.0
p	Number of χ^2 bins	16
δ	χ^2 threshold parameter	0.046
ξ^*	χ^2 threshold paramater	2.3

TABLE III. The coincidence windows used for the LIGO-TAMA300 search.

Parameter	Description	value
δt_{HT}	Timing between Hanford and TAMA	27.0 ms
δt_{LT}	Timing between Livingston and TAMA	35.0 ms
$\delta \mathcal{M}$	Chirp mass window	$0.05M_\odot$

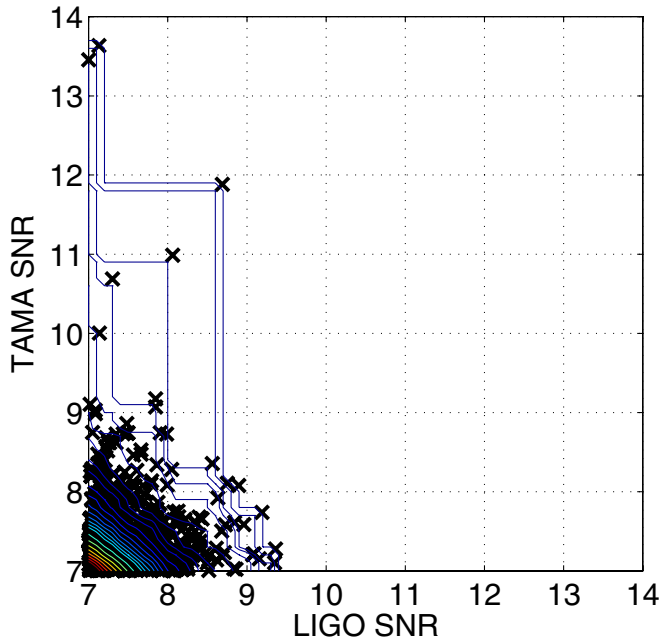


FIG. 2 (color online). The signal to noise ratios ρ_{LIGO} vs ρ_{TAMA} of the accidental coincident triggers using 100 time-shifts. The contours of constant false alarm probability are also shown.

To measure the sensitivity of the search, we perform a set of injections into both sets of data. The simulated waveforms added to the data consist of galactic binary neutron star inspiral signals. The majority of neutron stars in the Milky Way lie in the galactic bulge, which we take to have a radius of 4 kpc and height of 1.5 kpc. The sun is assumed to lie 8.5 kpc from the center of the galaxy. Further details of the galactic model used are available in Ref. [21]. The mass distribution is described in detail in Ref. [22]. Of the injections performed, 76% have an associated coincident trigger in the LIGO and TAMA300 detectors. The majority of the injections not detected have an effective distance at the TAMA300 site greater than TAMA300's range during DT8. However, there were also a few injections which were very poorly oriented for the LIGO detectors, and hence have a large effective distance, making them unobservable to LIGO. Finally, several injections produce triggers in both the LIGO and TAMA300 detectors but these fail our coincidence requirements. The SNRs of these triggers are close to threshold in TAMA300 and the injection parameters, in particular, the chirp mass, are recovered poorly. In Fig. 3 we plot the coincident triggers associated with injections superimposed on those from the time-shift analysis. This shows that triggers from the found injections are well separated from the accidental coincidences found in the time-shift analysis.

In Fig. 4, we plot the sensitivity of the search to injected Milky Way signals. For consistency with previous searches [7] we use N_G to represent the number of galaxies to which the search is sensitive. For this search, N_G is equivalent to

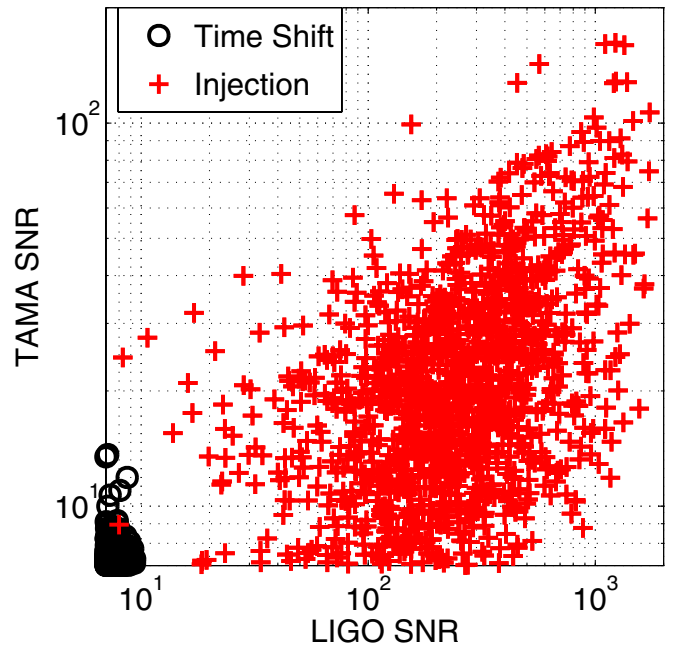


FIG. 3 (color online). The signal to noise ratios ρ_{LIGO} vs ρ_{TAMA} of the triggers associated with injections (+) and those from accidental coincidences arising in 100 time-shifts (o).

the fraction of Milky Way signals we are sensitive to. The figure shows the number of galaxies the search is sensitive to as a function of the threshold on the combined statistic given in Eq. (2). Thus, at threshold we are sensitive to a little more than three quarters of candidate sources in the galaxy. The efficiency curve is used later in determining the upper limit and associated systematic errors.

We analyze the S2/DT8 data using the pipeline described. The cumulative distribution of ρ_C of the coinci-

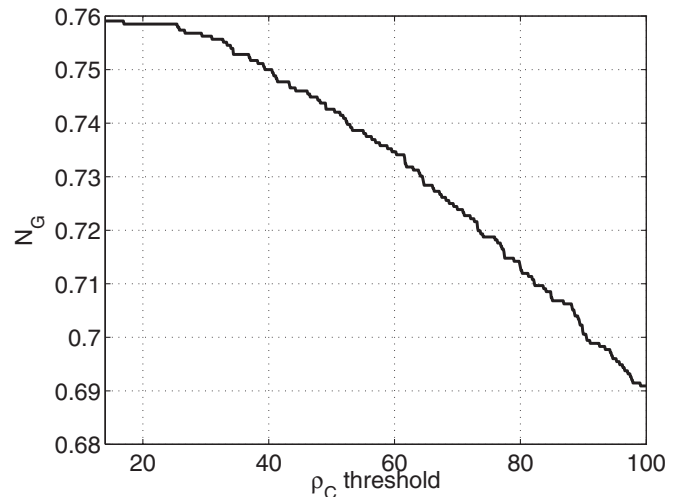


FIG. 4. The efficiency of the LIGO-TAMA300 joint analysis to simulated galactic inspiral events. The number of galaxies (N_G) to which the search is sensitive is plotted as a function of the threshold on the combined statistic $\rho_C (= \rho_{\text{LIGO}} + \rho_{\text{TAMA}})$.

dent triggers is shown in Fig. 5. On this plot, the expected number of triggers obtained from the time-shift analysis is shown, as well as the standard deviation of the number of triggers obtained in the time-shifts. The results of the analysis of the full data are overlaid on top of this. It is clear from the figure that the distribution of coincident triggers is consistent with the background estimated from time-shifts. There are no triggers with combined SNR greater than $\rho_{\max} = 15.3$. Therefore, we conclude that there is no evidence for gravitational wave signals in the LIGO-TAMA300 S2/DT8 data set.

Given the set of triggers displayed in Fig. 5 we can obtain an upper limit on the rate of binary neutron star coalescences per year per Milky Way Equivalent Galaxy (MWEG). (Although this search is only sensitive to galactic inspiral events, we maintain the standard ‘‘MWEG’’ [7] for describing the upper limit). We use the loudest event statistic [23], which makes use of the detection efficiency at the combined SNR of the loudest event in order to construct the upper limit. The 90% confidence frequentist upper limit is given by

$$\mathcal{R}_{90\%} = \frac{2.303 + \ln P_b}{TN_G(\rho_{\max})}. \quad (3)$$

In the above, T is the observation time of 584 h, P_b is the probability that all background triggers have a SNR less than ρ_{\max} , and N_G is the number of MWEGs the search is sensitive to at the combined SNR of the loudest event ρ_{\max} . N_G is determined from Fig. 4 to be 0.76 MWEG for $\rho_{\max} = 15.3$. Although the time-shift analysis provides us with an estimate of $P_b = 0.2$, we note that it is difficult to establish

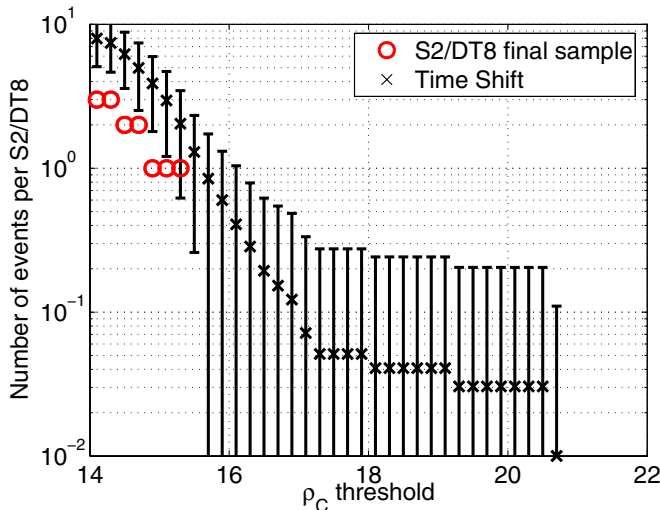


FIG. 5 (color online). The triggers from the analysis of the full LIGO-TAMA300 data set. The \times represent the expected background number of triggers at or above a given combined SNR ρ_C based on the 100 time-shifts performed. The bars indicate the standard deviation of the number of events, calculated from the time-shift results. The triggers from the final S2/DT8 data set are shown as \circ .

a systematic error associated with this estimate, and therefore take the conservative choice of setting $P_b = 1$. From these numbers, we obtain an upper limit of $\mathcal{R}_{90\%} = 45 \text{ y}^{-1} \text{ MWEG}^{-1}$.

The possible systematics which arise in a search for binary neutron stars are described in some detail in Ref. [7], and we will follow the analysis presented there to calculate the systematic errors for the above result. The most significant effects are due to the possible calibration inaccuracies of the detectors, the finite number of Monte Carlo injections performed, and the mismatch between our search templates and the actual waveform. We must also evaluate the systematic errors associated with the chosen astrophysical model of potential sources within the galaxy. All systematic effects in the analysis pipeline (such as less than perfect coverage of the template bank) are taken into account in the Monte Carlo estimation of the detection efficiency.

This search was sensitive to most, but not all, signals from the Milky Way. Thus, the specific model of the source distribution within the galaxy will affect the upper limit. The majority of the mass in the galaxy, and hence the potential sources, is concentrated near the galactic center. Therefore, our efficiency will be most affected by changing the distance from the sun to the center of the galaxy in the model. In this search, the sun’s galactocentric distance is assumed to be 8.5 kpc. Varying this distance between 7 and 10 kpc leads to a change in efficiency of 0.04 MWEG. Different models for NS-NS formation can lead to variations in the NS mass distribution. Based on simulations with a 50% reduction in the number of binary systems with masses in the range $1.5M_{\odot} < m_1, m_2 < 3.0M_{\odot}$, we can estimate the variation in N_G to be 0.01 MWEG.

Any calibration inaccuracy in TAMA300 could have a significant effect upon our efficiency. This is clear from Fig. 3 which shows a significant number of injections found in TAMA300 close to threshold. Two effects contribute to this calibration error: an overall normalization error (associated with the magnetic actuation strength uncertainty and its effect on calibration), and uncertainty in the frequency-dependent response. The error in the normalization is of order 5%, but the long-term drift is unknown, so we conservatively use 10% in this paper. The frequency-dependent error was estimated and shown to be $\ll 10\%$, so it is subsumed into the overall 10% error on the SNR of the triggers. This calibration uncertainty leads to a 0.02 MWEG effect on our efficiency. The majority of injections are observed well above threshold in the LIGO detectors, and consequently the calibration uncertainty of 8.5% in L1 and 4.5% in H1/H2 results in a smaller uncertainty in the efficiency of < 0.01 MWEG. The error in the efficiency measurement due to the finite number of injections performed is 0.01 MWEG. Differences between the theoretical waveforms used in matched filtering the data and the real waveforms would decrease the efficiency of

our search. Allowing for a 10% loss in SNR due to inaccuracies in the model waveform [24–26] leads to a $+0/-0.02$ MWEF effect on the efficiency. Combining these effects, we obtain an efficiency of $N_G = 0.76^{+0.05}_{-0.06}$. Taking the downward excursion on N_G , we obtain a conservative upper limit of

$$\mathcal{R}_{90\%} = 49 \text{ y}^{-1} \text{ MWEF}^{-1}. \quad (4)$$

This rate is substantially higher than the predicted astrophysical rate of $8.3 \times 10^{-5} \text{ y}^{-1} \text{ MWEF}^{-1}$ [27]. However, the rate limit obtained in this paper is comparable with the rate limit of $47 \text{ y}^{-1} \text{ MWEF}^{-1}$ obtained from the LIGO-only S2 search [7], which was performed on a complementary data set. Since these searches were performed on independent data sets, if astrophysically relevant, these upper limits could then be combined to produce the best possible limit. The fact that the LIGO S2 and LIGO-TAMA300 S2/DT8 limits are so similar demonstrates that the overall sensitivities of the two searches are very nearly equal. This is achieved despite the fact that the TAMA300 detector was less sensitive than LIGO during S2/DT8. The high duty cycle of TAMA300 (over 80%) compensates for the reduced sensitivity, and leads to a similar overall result.

In this paper, we have presented the methods and results from the first multicollaboration, network search for gravitational waves from inspiralling binary systems using large scale interferometers. The search was performed using a trigger exchange method, requiring coincidence in both the end time and chirp mass of triggers between instruments. Using this method, we have performed all necessary steps of the analysis, including time-shifts, signal injections and the calculation of the upper limit. The joint, coincidence search presented here is a natural first step in any network analysis. The methods developed during this search will be

applied in future network searches. Indeed, the experience gained during this joint search is being used in subsequent LIGO Scientific Collaboration searches of LIGO and GEO data. Furthermore, a trigger exchange coincidence analysis is being developed as the first stage of a future joint LIGO-Virgo analysis. The optimal network search would likely involve a fully coherent analysis [20] of the detectors' data streams around the times of coincident events. A coherent follow-up to the coincidence method presented in this paper would be included in future analyses of LIGO and TAMA300 data with improved sensitivity, or in joint analyses of the planned second generation detectors such as advanced LIGO [28] in U.S. and LCGT [29] in Japan.

The authors gratefully acknowledge the support of the United States National Science Foundation for the construction and operation of the LIGO Laboratory and the Particle Physics and Astronomy Research Council of the United Kingdom, the Max-Planck-Society and the State of Niedersachsen/Germany for support of the construction and operation of the GEO600 detector. The authors also gratefully acknowledge the support of the research by these agencies and by the Australian Research Council, the Natural Sciences and Engineering Research Council of Canada, the Council of Scientific and Industrial Research of India, the Department of Science and Technology of India, the Spanish Ministerio de Educacion y Ciencia, the John Simon Guggenheim Foundation, the Leverhulme Trust, the David and Lucile Packard Foundation, the Research Corporation, and the Alfred P. Sloan Foundation. TAMA research is supported by a Grant-in-Aid for Scientific Research on Priority Areas (415) of the Ministry of Education, Culture, Sports, Science and Technology of Japan. This work was also supported in part by JSPS Grant-in-Aid for Scientific Research Nos. 14047214 and 12640269.

-
- [1] B. Abbot *et al.* (LIGO Scientific Collaboration), Nucl. Instrum. Methods Phys. Res., Sect. A **517**, 154 (2004).
 - [2] R. Takahashi (TAMA Collaboration), Classical Quantum Gravity **21**, S403 (2004); M. Ando *et al.* (TAMA Collaboration), Phys. Lett. **86**, 3950 (2001).
 - [3] B. Willke *et al.*, Classical Quantum Gravity **21**, S417 (2004).
 - [4] F. Acernese *et al.* (VIRGO Collaboration), Classical Quantum Gravity **21**, S385 (2004).
 - [5] B. Abbott *et al.* (LIGO Scientific Collaboration), Phys. Rev. D **69**, 122001 (2004).
 - [6] H. Tagoshi *et al.* (TAMA Collaboration), Phys. Rev. D **63**, 062001 (2001).
 - [7] B. Abbott *et al.* (LIGO Scientific Collaboration), Phys. Rev. D **72**, 082001 (2005).
 - [8] TAMA Collaboration (to be published).
 - [9] Z.A. Allen *et al.* (International Gravitational Event Collaboration), Phys. Rev. Lett. **85**, 5046 (2000).
 - [10] B. Abbott *et al.* (LIGO Scientific Collaboration and TAMA Collaboration), Phys. Rev. D **72**, 122004 (2005).
 - [11] S. Fairhurst (for the LIGO Scientific Collaboration), H. Takahashi (for the TAMA Collaboration), Classical Quantum Gravity **22**, S1109 (2005).
 - [12] H. Takahashi, H. Tagoshi, and the TAMA Collaboration, Classical Quantum Gravity **21**, S697 (2004).
 - [13] B.J. Owen, Phys. Rev. D **53**, 6749 (1996); B.J. Owen and B.S. Sathyaprakash, Phys. Rev. D **60**, 022002 (1999).
 - [14] B. Allen, W.G. Anderson, P.R. Brady, D.A. Brown, and J.D.E. Creighton, gr-qc/0509116.
 - [15] LSC Algorithm Library software packages LAL and LALAPPS, the CVS tag versions INSPIRAL-LIGO-TAMA-20050504 of which were used in this analysis. <http://www.lsc.org>

- lsc-group.phys.uwm.edu/daswg/projects/lal.html.
- [16] B. Allen, Phys. Rev. D **71**, 062001 (2005).
- [17] T. Tanaka and H. Tagoshi, Phys. Rev. D **62**, 082001 (2000).
- [18] H. Takahashi and H. Tagoshi *et al.* (TAMA Collaboration and LISM Collaboration), Phys. Rev. D **70**, 042003 (2004).
- [19] E. Amaldi *et al.*, Astron. Astrophys. **216**, 325 (1989); P. Astone *et al.*, Phys. Rev. D **59**, 122001 (1999).
- [20] A. Pai, S. Dhurandhar, and S. Bose, Phys. Rev. D **64**, 042004 (2001).
- [21] C. Kim, V. Kalogera, and D.R. Lorimer, Astrophys. J. **584**, 985 (2003).
- [22] K. Belczynski, V. Kalogera, and T. Bulik, Astrophys. J. **572**, 407 (2002).
- [23] P.R. Brady, J.D.E. Creighton, and A.G. Wiseman, Classical Quantum Gravity **21**, S1775 (2004).
- [24] T.A. Apostolatos, Phys. Rev. D **52**, 605 (1995).
- [25] S. Droz and E. Poisson, Phys. Rev. D **56**, 4449 (1997).
- [26] S. Droz, Phys. Rev. D **59**, 064030 (1999).
- [27] V. Kalogera *et al.*, Astrophys. J. **601**, L179 (2004); **614**, L137(E) (2004).
- [28] P. Fritschel, *Second Generation Instruments for the Laser Interferometer Gravitational Wave Observatory (LIGO)*, Proc. SPIE Vol. 4856–39 (Waikoloa, HI, 2002), p. 282–291.
- [29] K. Kuroda *et al.*, Int. J. Mod. Phys. D **8**, 557 (1999); K. Kuroda *et al.*, Classical Quantum Gravity **20**, S871 (2003); T. Uchiyama *et al.*, Classical Quantum Gravity **21**, S1161 (2004).